scientific reports

OPEN

Analytical solutions of PDEs by unique polynomials for peristaltic flow of heated Rabinowitsch fluid through an elliptic duct

Salman Akhtar[1✉], Muhammad Hasnain Shahzad[2], Sohail Nadeem[1], Aziz Ullah Awan[2], Shahah Almutairi[3], Hassan Ali Ghazwani[4] & Mohamed Mahmoud Sayed[5]

In this research, we have considered the convective heat transfer analysis on peristaltic flow of Rabinowitsch fluid through an elliptical cross section duct. The Pseudoplastic and Dilatant characteristics of non-Newtonian fluid flow are analyzed in detail. The Rabinowitsch fluid model shows Pseudoplastic fluid nature for $\sigma > 0$ and Dilatant fluid behaviour for $\sigma < 0$. The governing equations are transformed to dimensionless form after substituting pertinent parameters and by applying the long wavelength approximation. The non-dimensional momentum and energy equations are solved analytically to obtain the exact velocity and exact temperature solutions of the flow. A novel polynomial of order six having ten constants is introduced first time in this study to solve the energy equation exactly for Rabinowitsch fluid flow through an elliptic domain. The analytically acquired solutions are studied graphically for the effective analysis of the flow. The flow is found to diminish quickly in the surrounding conduit boundary for Dilatant fluid as compared to the Pseudoplastic fluid. The temperature depicted the opposite nature for Pseudoplastic and Dilatant fluids. The flow is examined to plot the streamlines for both Pseudoplastic and Dilatant fluids by rising the flow rate.

List of symbols

(X, Y, Z)	Cartesian coordinates
d	Wave amplitude
D_h	Hydraulic diameter
T_b	Bulk temperature
a_0, b_0	Semi axes of ellipse
δ	Aspect-ratio
μ	Dynamic viscosity
σ	Coefficient of pseudoplasticity
(U, V, W)	Velocity components
λ	Wavelength
e	Eccentricity
T_w	Wall temperature
c	Velocity of propagation
ϕ	Occlusion
B_r	Brinkman number

[1]Department of Mathematics, Quaid-I-Azam University, Islamabad 4532044000, Pakistan. [2]Department of Mathematics, University of the Punjab, Lahore, Pakistan. [3]Mathematics Department, Faculty of Sciences, Northern Border University, Arar 1321, Saudi Arabia. [4]Department of Mechanical Engineering, Faculty of Engineering, Jazan University, P.O box 45124, Jazan, Kingdom of Saudi Arabia. [5]Architectural Engineering Department, Faculty of Engineering and Technology, Future University in Egypt, New Cairo 11835, Egypt. ✉email: sakhtar@math.qau.edu.pk
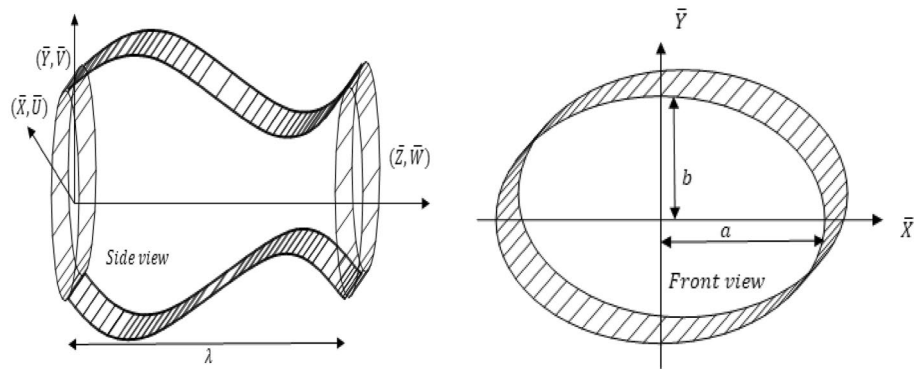
Figure 1. Geometry of Elliptic Duct.

The process in which fluid flows across a conduit by the sinusoidal fluctuating boundaries is known as Peristalsis. The fluid propels by the means of deformation of the walls parallel to the axis of channel in peristaltic flow. The wide applications of peristaltic flow in the industrial area, physiological and engineering fields like corrosive fluid transport, blood pumps in heart lungs machines, blood flow in small vessels makes it much important. Due to these many applications numerous researchers has been studying the peristaltic flow via various conduits. Bohm and Friedrich studied the flow of viscoelastic fluids under peristaltic wall deformation of channel by considering an assumption of small Reynold number[1]. Siddiqui and Schwarz provided analytical study of the Second-grade fluid flow through axisymmetric tubes with sinusoidally vibrating walls[2]. Eytan et al. described the peristaltic flow via narrowed conduit under the application of embryo transport within the uterine aperture[3]. Tsiklauri and Beresnev had considered the flow of Maxwell fluid across a circular channel with peristaltic movement of the boundary[4]. Rao and Mishra explained the asymmetric channel flow in addition to viscous effects and without neglecting the curvature effects[5]. Reddy et al. analyzed fluid flow due to fluctuating walls of rectangular shape channel by considering long wavelength approximation[6]. The fractional model of Maxwell fluid is utilized to study the visco-elastic fluid flow inside a sinusoidal wavy conduit by Tripathi et al.[7].

Ali et al. provided the analysis of temperature distribution within a curved wavy conduit[8]. Akbar et al.[9] examined the entropy generation and MHD influences on peristaltic flow. Maraj and Nadeem[10] interpreted the curved channel peristaltic flow of non-Newtonian Rabinowitsch fluid. Hayat et al.[11] explained the entropy interpretation of peristaltic flow of nanofluid in a rotating frame. Rashid et al.[12] explained the Williamson fluid flow via curved conduit under the influence of magnetic and peristaltic effects. Saleem et al.[13] studied the Casson fluid to highlight the non-Newtonian nature of fluid via duct with elliptical cross section and fluid flows due to peristaltic effects. McCash et al.[14] provided the analysis of Newtonian fluid flow through elliptical duct affected by cilia. Asha and Beleri[15] highlighted the nanofluid effects on non-Newtonian Carreau model for an axially symmetric inclined conduit by contemplating the Joule heating effect. Riaz et al.[16] gave the analysis of solid particles influence on the peristaltically flowing Jeffery fluid across eccentric annuli. Vaidya et al.[17,18] studied the influence of variable liquid and rheological characteristics on peristaltic flow of Rabinowitsch fluid across an inclined channel. The variables properties and application of peristaltic flow of non-Newtonian Rabinowitsch fluid under various effects is discussed by many researchers[19–22].

The heat transfer effects on fluid flowing through different channels are studied by many researchers. The peristaltic flow of heated magnetohydrodynamic fluid under partial slip influence is analyzed by Nadeem and Akram[23]. Akbar and Butt[24] provided the analytical study of nanofluid flow in curved tube with vibrating walls. Bibi and Xu[25] presented the heat transfer in a nanofluid flow through a horizontal conduit with MHD effects. Raza et al.[26] gave the study of water-based nanofluid for various shaped nanoparticles in an asymmetric conduit having permeable boundary under magnetic effects. The influence of heat flux and endoscope on non-Newtonian Jeffery fluid movement across concentric symmetric tubes due to peristaltic motion of walls is discussed by Abd-Alla and Abo-Dahab[27]. Abbasi et al.[28] examined the nanofluids flow under the peristaltic and electroosmotic effects via asymmetric narrow channel. Li et al.[29] studied the peristaltic movement of non-Newtonian nanofluid by utilizing Jeffery fluid model under the hall effects and viscous dissipation. Some of the recent literature work that highlights the peristaltic flow, pseudo plastic flow characteristics, MHD impacts and chemical reactions on a channel flow problem are given as[30–33].

In this research, we have studied the heated Rabinowitsch fluid flow across a duct of elliptical cross section. The published literature and researchers clearly highlight that there is no research on Peristaltic flow of heated Rabinowitsch fluid inside an elliptic duct. The non-Newtonian fluid flow is studied through a channel with sinusoidally fluctuating boundary walls. The velocity and heat transfer effects on fluid flow are analyzed. A unique polynomial is involved to obtain the solution of temperature. The dilatant and pseudoplastic characteristics of the Rabinowitsch fluid are examined.

Mathematical formulation

Consider the flow of a heated Rabinowitsch fluid through a duct having elliptical cross section. The elliptic shape conduit is studied with sinusoidally fluctuating walls. The mathematical study in completed by utilizing cartesian coordinates (X, Y, Z). The sinusoidally deformed walls are taken as[34] and the geometrical model is given by Fig. 1

$$a(Z, t) = a_0 + d \sin\left(\frac{2\pi}{\lambda}(Z - ct)\right), \tag{1-a}$$

$$b(Z, t) = b_0 + d \sin\left(\frac{2\pi}{\lambda}(Z - ct)\right), \tag{1-b}$$

The governing equations of incompressible fluids are

$$\frac{\partial U}{\partial X} + \frac{\partial V}{\partial Y} + \frac{\partial W}{\partial Z} = 0, \tag{2}$$

$$\rho\left(\frac{\partial U}{\partial t} + U\frac{\partial U}{\partial X} + V\frac{\partial U}{\partial Y} + W\frac{\partial U}{\partial Z}\right) = -\frac{\partial P}{\partial X} + \frac{\partial \tau_{XX}}{\partial X} + \frac{\partial \tau_{XY}}{\partial Y} + \frac{\partial \tau_{XZ}}{\partial Z}, \tag{3}$$

$$\rho\left(\frac{\partial V}{\partial t} + U\frac{\partial V}{\partial X} + V\frac{\partial V}{\partial Y} + W\frac{\partial V}{\partial Z}\right) = -\frac{\partial P}{\partial Y} + \frac{\partial \tau_{YX}}{\partial X} + \frac{\partial \tau_{YY}}{\partial Y} + \frac{\partial \tau_{YZ}}{\partial Z}, \tag{4}$$

$$\rho\left(\frac{\partial W}{\partial t} + U\frac{\partial W}{\partial X} + V\frac{\partial W}{\partial Y} + W\frac{\partial W}{\partial Z}\right) = -\frac{\partial P}{\partial Z} + \frac{\partial \tau_{ZX}}{\partial X} + \frac{\partial \tau_{ZY}}{\partial Y} + \frac{\partial \tau_{ZZ}}{\partial Z}, \tag{5}$$

$$\rho c_p\left(\frac{\partial T}{\partial t} + U\frac{\partial T}{\partial X} + V\frac{\partial T}{\partial Y} + W\frac{\partial T}{\partial Z}\right) = k\left(\frac{\partial^2 T}{\partial X^2} + \frac{\partial^2 T}{\partial Y^2} + \frac{\partial^2 T}{\partial \bar{z}^2}\right) + \left(\tau_{XX}\frac{\partial U}{\partial X} + \tau_{XY}\frac{\partial U}{\partial Y} + \tau_{XZ}\frac{\partial U}{\partial Z}\right)$$
$$+ \left(\tau_{YX}\frac{\partial V}{\partial X} + \tau_{YY}\frac{\partial V}{\partial Y} + \tau_{YZ}\frac{\partial V}{\partial Z}\right) + \left(\tau_{ZX}\frac{\partial W}{\partial X} + \tau_{ZY}\frac{\partial W}{\partial Y} + \tau_{ZZ}\frac{\partial W}{\partial Z}\right), \tag{6}$$

The boundary conditions corresponding to above equations are

$$W = 0, T = 0 \, for \, \frac{X^2}{a^2} + \frac{Y^2}{b^2} = 1 \tag{7}$$

The Rabinowitsch fluid stress tensor is provided as[17]

$$\tau_{YZ} + \sigma \tau_{YZ}^3 = \mu\frac{\partial W}{\partial Y}, \tag{8}$$

where, σ is coefficient of pseudoplasticity. The Rabinowitsch fluid shows Pseudoplastic, Newtonian, Dilatant behaviour for $\sigma > 0, \sigma = 0, \sigma < 0$ respectively.

The transformations relate the fixed (unsteady) and wave (steady) frames are given following

$$U = u, V = v, W - c = w,$$
$$P = p, X = x, Y = y, z = Z - ct, \tag{9}$$

The dimensionless variables to transform the equations into non-dimensional form

$$\bar{x} = \frac{x}{D_h}, \bar{y} = \frac{y}{D_h}, \bar{z} = \frac{z}{\lambda}, \bar{t} = \frac{ct}{\lambda},$$
$$\bar{a} = \frac{a}{D_h}, \delta = \frac{b_0}{a_0}, \bar{p} = \frac{D_h^2 p}{\mu\lambda c}, \phi = \frac{d}{b_0},$$
$$\bar{b} = \frac{b}{D_h}, \bar{u} = \frac{\lambda u}{D_h c}, \bar{v} = \frac{\lambda v}{D_h c}, \bar{w} = \frac{w}{c}, \tag{10}$$
$$\bar{\sigma} = \frac{\sigma c^2 \mu^2}{D_h^2}, \theta = \frac{T - T_w}{T_b - T_w}, \bar{s}_{ij} = \frac{D_h}{c\mu_f}s_{ij},$$
$$B_r = \frac{\mu u_0^2}{k(T_b - T_w)},$$

where, D_h is the hydraulic diameter of the ellipse and

$$D_h = \frac{\pi b_0}{E(e)}. \tag{11}$$

e is known as the eccentricity of the ellipse such that $0 < e < 1$ and $e = \sqrt{1 - \delta^2}$

$$E(e) = \int\limits_0^{\frac{\pi}{2}} \sqrt{1 - e^2 Sin^2(\alpha)} d\alpha. \tag{12}$$

By applying long wavelength approximation together with the transformation given in (9) and non-dimensional variables by ignoring dash notation provided in (10), Eqs. (2)-(7) takes the form

$$\frac{\partial p}{\partial x} = 0, \tag{13}$$

$$\frac{\partial p}{\partial y} = 0, \tag{14}$$

$$\frac{\partial p}{\partial z} + \frac{\partial \tau_{xz}}{\partial x} + \frac{\partial \tau_{yz}}{\partial y} = 0, \tag{15}$$

$$\frac{\partial^2 \theta}{\partial x^2} + \frac{\partial^2 \theta}{\partial y^2} + B_r \left[\tau_{xz} \frac{\partial w}{\partial x} + \tau_{yz} \frac{\partial w}{\partial y} \right] = 0, \tag{16}$$

The corresponding dimensionless boundary conditions are

$$w = 0, \theta = 0 \frac{x^2}{a^2} + \frac{y^2}{b^2} = 1, \tag{17}$$

The expression (1-a) and (1-b) take the form

$$a = \frac{E(e)}{\pi} \left(\frac{1}{\delta} + \phi Sin(2\pi z) \right), \tag{18-a}$$

$$b = \frac{E(e)}{\pi} (1 + \phi \sin(2\pi z)), \tag{18-b}$$

The dimensionless form of extra stress tensor for Rabinowitsch fluid is

$$\tau_{yz} + \sigma.\left(\tau_{yz} \right)^3 = \frac{\partial w}{\partial y}, \tag{19}$$

Exact solution
Axial velocity.
The following Eq. (20) represents the solution of Eq. (15) with the boundary conditions $\tau_{xz} = 0$ at $x = 0$ and $\tau_{yz} = 0$ at $y = 0$.

$$\tau_{xz} = \frac{\partial p}{\partial z} \frac{x}{2} \text{and} \tau_{yz} = \frac{\partial p}{\partial z} \frac{y}{2}, \tag{20}$$

The velocity solution is obtained by using Eq. (20) and direct integration of Eq. (19) as

$$w(x, y) = \frac{b^2}{4} \frac{\partial p}{\partial z} \left(\frac{x^2}{a^2} + \frac{y^2}{b^2} - 1 \right) + \frac{\sigma b^4}{32} \left(\frac{x^2}{a^2} + \frac{y^2}{b^2} - 1 \right) \left(-\frac{x^2}{a^2} + \frac{y^2}{b^2} + 1 \right). \tag{21}$$

The volumetric flow rate is attained by integrating the Eq. (21) over elliptic domain

$$q(z) = -\frac{ab^3 \pi \frac{\partial p}{\partial z}}{64} \left(8 + b^2 \left(\frac{\partial p}{\partial z} \right)^2 \sigma \right) \tag{22}$$

The mathematical expression for pressure gradient is attained by utilizing the equation $q(z) = Q - \int\limits_0^1 abdz$,

$$\frac{dp}{dz} = \frac{1}{3ab^5 \sigma \left(18\pi a^2 b^{10} (L - Q)\sigma^2 + \pi \sqrt{6a^4 b^{20} \sigma^3 (a^2 b^4 \pi^2 + 54(L - Q)^2 \sigma)} \right)^{\frac{1}{3}}}$$

$$\times \left[2a^2 b^8 (6\pi)^{2/3} \sigma - 2 \left\{ 6^{1/3} \left(18a^2 b^{10} (L - Q)\sigma^2 + \sqrt{6a^4 b^{20} \sigma^3 (a^2 b^4 \pi^2 + 54(L - Q)^2 \sigma)} \right)^{\frac{2}{3}} \right\} \right], \tag{23}$$

where, $L = \int\limits_0^1 abdz.$

The expression for pressure rise is obtained as

$$\triangle p = \int_0^1 \frac{dp}{dz},$$

Temperature profile.   The solution of temperature is attained by using the method provided in[35]. It is obtained by utilizing the following polynomial

$$\theta(x, y) = c_1 x^6 + c_2 y^6 + c_3 x^4 + c_4 y^4 + c_5 x^2 + c_6 y^2 + c_7 x^4 y^4 + c_8 x^2 y^2 + c_9 \left(x^4 y^2 - x^2 y^4\right) + c_{10}, \quad (24)$$

By setting the polynomial in Eq. (16) and taking coefficient of x^4, x^2, x^0, y^4, y^2, y^0 equal to zero, we have

$$-\frac{b^4 B_r \sigma}{16 a^4} \left(\frac{dp}{dz}\right)^4 + 30 c_1 + 12 y^2 c_7 + 2 c_9 = 0, \quad (25)$$

$$\frac{1}{16} B_r \left(\frac{dp}{dz}\right)^4 \sigma + 30 c_2 + 12 x^2 c_7 - 2 c_9 = 0, \quad (26)$$

$$\frac{b^2 B_r}{4 a^2} \left(\frac{dp}{dz}\right)^2 + \frac{b^4 B_r \sigma}{16 a^2} \left(\frac{dp}{dz}\right)^4 + 12 c_3 + 12 y^4 c_7 + 2 c_8 = 0, \quad (27)$$

$$\frac{B_r}{4} \left(\frac{dp}{dz}\right)^2 + 12 c_4 + 12 x^4 c_7 + 2 c_8 = 0, \quad (28)$$

$$c_5 + c_6 = 0, \quad (29)$$

Moreover, using boundary condition and comparing the coefficients of x^8, x^6, x^4, x^2, x^0, we obtain

$$\frac{b^4 c_7}{a^4} = 0, \quad (30)$$

$$c_1 - \frac{b^6 c_2}{a^6} - \frac{2 b^4 c_7}{a^2} - \frac{b^2 c_9}{a^2} - \frac{b^4 c_9}{a^4} = 0, \quad (31)$$

$$\frac{3 b^6 c_2}{a^4} + c_3 + \frac{b^4 c_4}{a^4} + b^4 c_7 - \frac{b^2 c_8}{a^2} + b^2 c_9 + \frac{2 b^4 c_9}{a^2} = 0, \quad (32)$$

$$-\frac{3 b^6 c_2}{a^2} - \frac{2 b^4 c_4}{a^2} + c_5 - \frac{b^2 c_6}{a^2} + b^2 c_8 - b^4 c_9 = 0, \quad (33)$$

$$b^6 c_2 + b^4 c_4 + b^2 c_6 + c_{10} = 0, \quad (34)$$

The solution of temperature is acquired by solving the Eqs. (25)–(34) simultaneously and putting the value of constants in Eq. (24) as

$$\theta(x, y) = \frac{-a^2 b^2}{960 a^4 \left(a^2 + b^2\right) \left(a^4 + 6 a^2 b^2 + b^4\right) \left(a^4 + 14 a^2 b^2 + b^4\right)}$$

$$\times \left[B_r \left(\frac{dp}{dz}\right)^2 \left(\frac{x^2}{a^2} + \frac{y^2}{b^2} - 1\right) \left(\left(20 a^2 \left(a^4 + 14 a^2 b^2 + b^4\right) \left(b^6 x^2 \right.\right.\right.\right.$$

$$+ a^6 \left(b^2 + y^2\right) + a^2 b^4 \left(b^2 + 6 x^2 + 5 y^2\right) + a^4 b^2 \left(10 b^2 + 5 x^2 + 6 y^2\right)\right)$$

$$+ \left(\frac{dp}{dz}\right)^2 \left(b^4 \left(a^4 \left(2 a^8 + 61 a^6 b^2 + 355 a^4 b^4 + 59 a^2 b^6 + 3 b^8\right)\right.\right.$$

$$+ a^2 \left(a^2 + b^2\right) \left(26 a^6 + 231 a^4 b^2 + 60 a^2 b^4 + 3 b^6\right) x^2 - 2 \left(a^2 + b^2\right) \left(14 a^2 + b^2\right) \left(a^4 + 6 a^2 b^2 + b^4\right) x^4\right)$$

$$+ a^2 b^2 \left(a^2 + b^2\right) \left(2 a^8 + 35 a^6 b^2 + 124 a^4 b^4 - a^2 b^6 - 2 \left(a^2 - b^2\right) \left(a^4 + 6 a^2 b^2 + b^4\right) x^2\right) y^2$$

$$+ 2 a^4 \left(a^2 + b^2\right) \left(a^2 + 14 b^2\right) \left(a^4 + 6 a^2 b^2 + b^4\right) y^4\right) \sigma\right)\right]$$
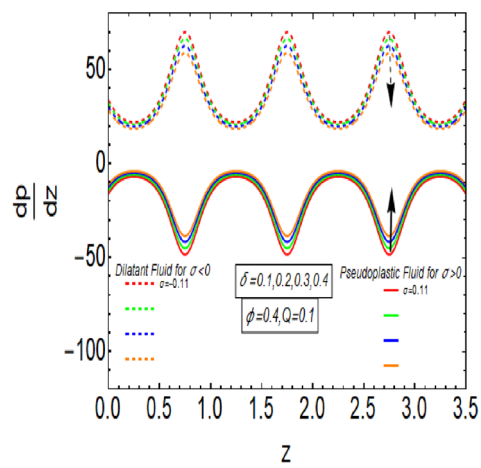
$$(35)$$
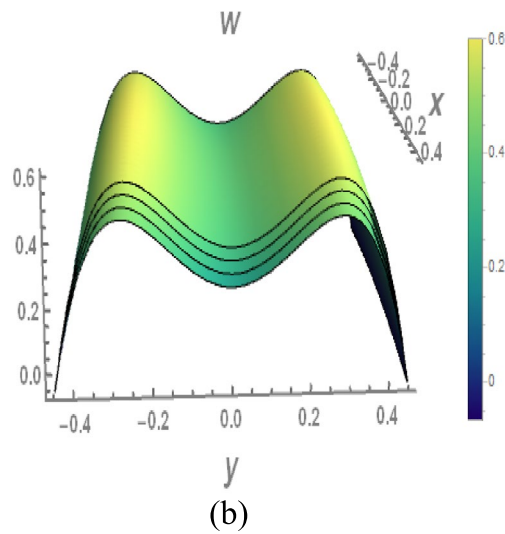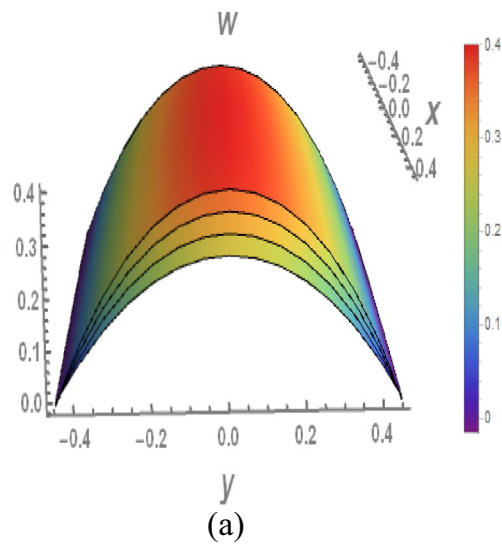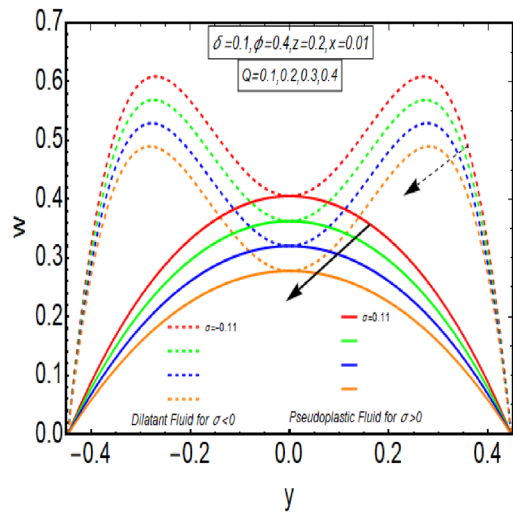
Figure 2. Velocity Profile for Q with $\sigma > 0$ and $\sigma < 0$. (**a**) $\sigma > 0$, (**b**) $\sigma < 0$.
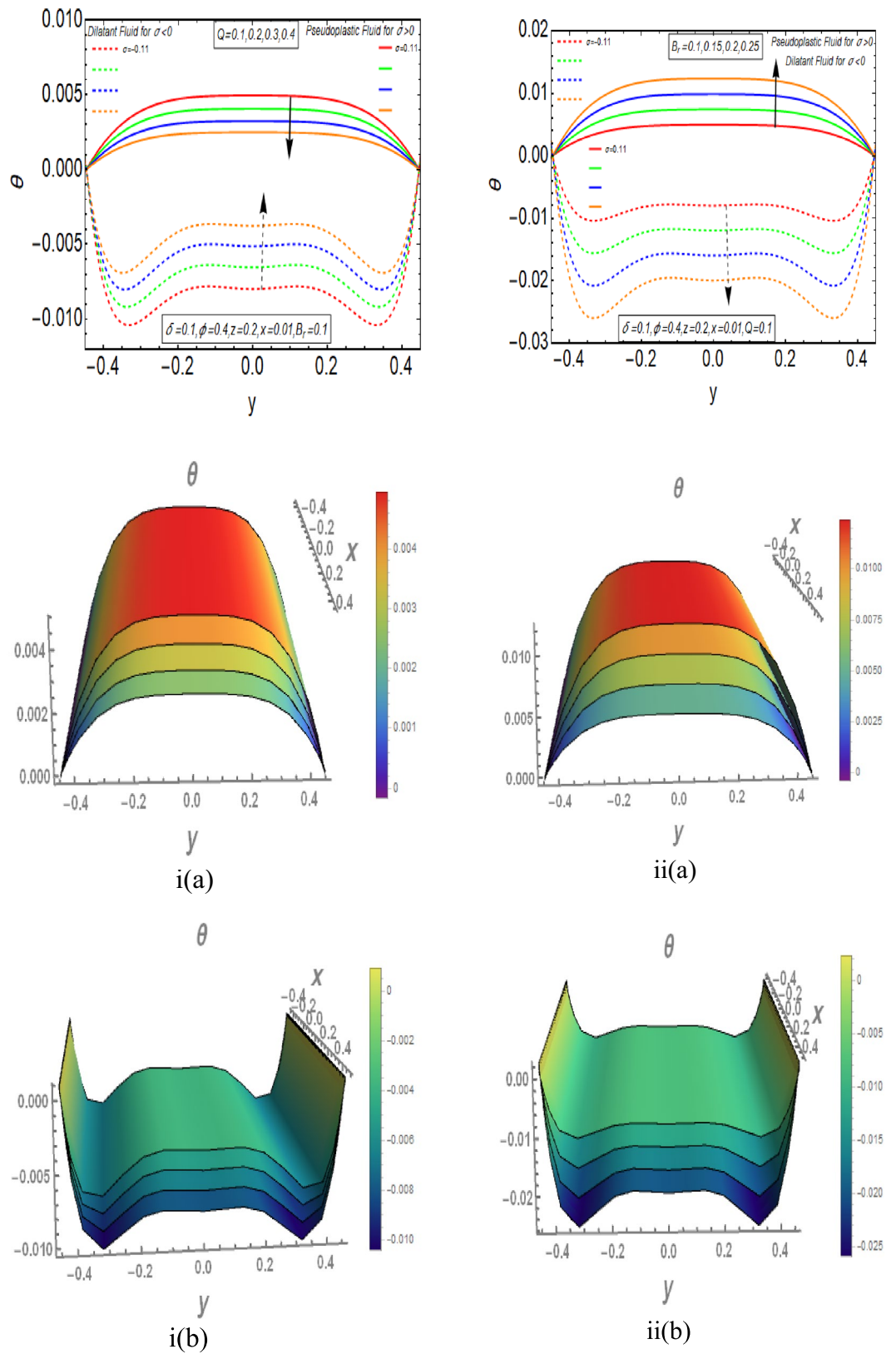
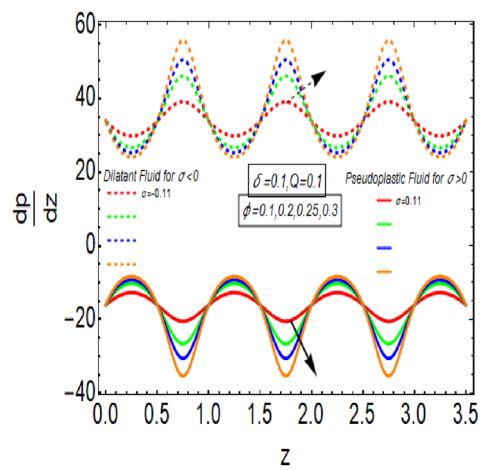**Figure 3.** (**i**) Temperature graph for Q with $\sigma > 0$ and $\sigma < 0$, i(**a**) $\sigma > 0$, i(**b**) $\sigma < 0$. (**ii**)Temperature graph for Br with $\sigma > 0$ and $\sigma < 0$, ii(**a**) $\sigma > 0$, ii(**b**) $\sigma < 0$.
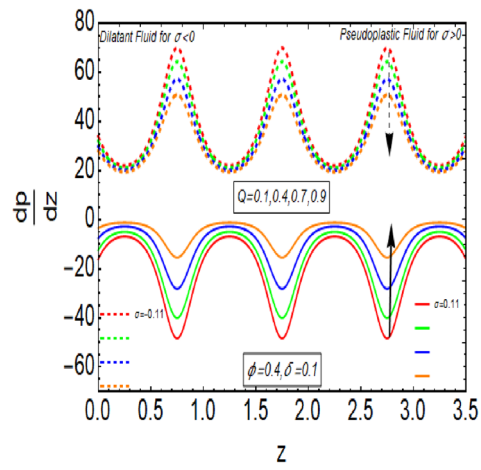
(a)

(b)

(c)

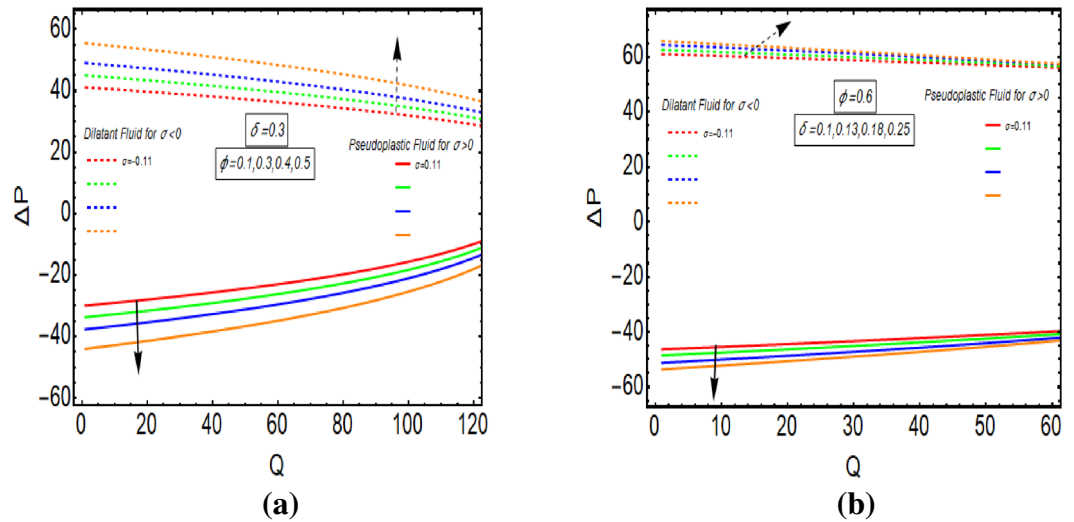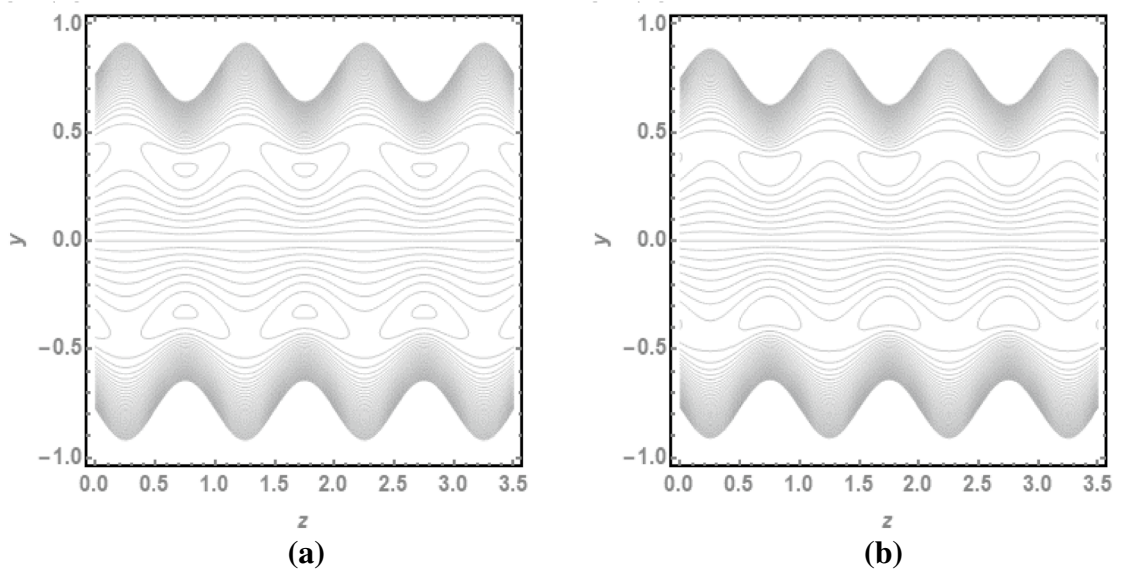**Figure 4.** (**a**) $\frac{dp}{dz}$ for Q with $\sigma > 0$ and $\sigma < 0$. (**b**) $\frac{dp}{dz}$ for δ with $\sigma > 0$ and $\sigma < 0$. (**c**) $\frac{dp}{dz}$ for φ with $\sigma > 0$ and $\sigma < 0$.

Figure 5. (**a**) Pressure rise for φ with $\sigma > 0$ and $\sigma < 0$. (**b**) Pressure rise for δ with $\sigma > 0$ and $\sigma < 0$.

Figure 6. (**a**) Streamline for $Q = 1.4$ and $\sigma > 0$. (**b**) Streamline for $Q = 1.6$ and $\sigma > 0$.

Results and discussion

The graphical analysis of analytically attained results in earlier fragment is presented in this section. This analysis provides an effective study and better understanding of the physical aspects of peristaltic motion of Rabinowitsch fluid flow across elliptic duct. The effect of different physical constraints on the flow velocity, temperature distribution, pressure gradient and pressure rise are discussed. The three-dimensional graphs of velocity and temperature distribution are provided in this graphical examination. Figure 2 has a graphical analysis of the flow velocity for rising values of Q. It explains that the velocity of flowing fluid decreases for rapid flow. The velocity of Dilatant fluid has greatest magnitude near the wall of the conduit and diminishes very quickly towards the walls to approach its lowest value. But velocity of Pseudoplastic fluid is maximum at mean of conduit and diminishes gradually towards the walls to get its smallest magnitude. The graph of Dilatant fluid grows fast as compared to the Pseudoplastic fluid. Moreover, flow velocity of Pseudoplastic and Dilatant fluids are same on the axis of channel.

The Fig. 3i,ii provides the information about the behavior of temperature profile of Rabinowitsch fluid flow. Figure 3i shows the belonging of temperature profile with flow rate Q. The magnitude of temperature diminishes by improving the values of flow rate Q for Pseudoplastic behaviour of Rabinowitsch fluid. It remains same near the mid of channel and declines quickly close to the boundary walls. But the Rabinowitsch fluid shows opposite nature for its Dilatant behavior. Figure 3ii depicts the effect of Brinkman number on temperature graph. It delineates that temperature profile reduces for enlarging values of Brinkman number in the case of Dilatant fluid. It rises rapidly in surrounding of deformed wall and remains similar away from it. The temperature of Pseudoplastic fluid enhances by incrementing the values of Brinkman number. The temperature graph of Pseudoplastic and Dilatant fluid shows opposite behavior for increasing magnitude of B_r.
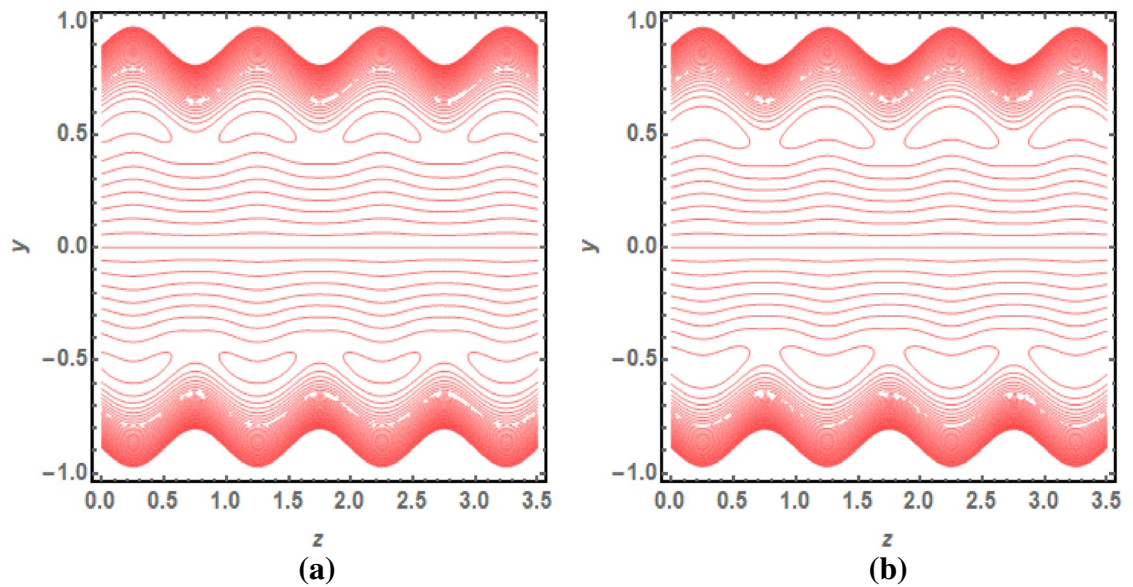
Figure 7. (**a**) Streamline for $Q = 1.4$ and $\sigma < 0$. (**b**) Streamline for $Q = 1.6$ and $\sigma < 0$.

Figure 4a–c reveals the dependence of pressure gradient on the flow rate, aspect ratio and occlusion. Figure 4a explains that pressure gradient graph gets down by increasing the flow rate for Dilatant behavior whereas it gets height for Pseudoplastic behavior of Rabinowitsch fluid. Figure 4b represents that the pressure gradient has larger magnitude by increasing the values of δ for the Pseudoplastic fluid. But it gives reverse behaviour in the cases of Dilatant fluid. Figure 4c indicates the nature of the pressure gradient graph for growing values of φ. Its graph is increasing with $0 < z < 0.5$ and it diminishes with $0.5 < z < 1$ for the larger values of φ in the case of Pseudoplastic fluid. It shows similar behaviour for other values z. But the pressure gradient has opposite nature for Dilatant fluid. The pressure gradient has maximum and minimum values for Dilatant and Pseudoplastic fluid at $z = n + 0.75$, n is whole number, respectively.

Figure 5a,b provides the graphical representation of pressure rise for δ and φ. Figure 5a reveals the enhancing behaviour of pressure rise by incrementing the values of δ for Dilatant nature. But it has opposite behavior for pseudoplastic nature of fluid. Figure 5b depicts the increasing graph of pressure rise for improving values of φ. It shows that Dilatant and Pseudoplastic fluids has opposite nature as a function of φ. The value of Δp gets closer to each other for increasing values of Q. Figures 6a, 7b provides the streamline analysis of Rabinowitsch fluid through an elliptic duct under the peristaltic motion. Figure 6a,b shows the generation of trappings for various values of flow rate. They clarify that number and size of vortices reduces for higher values of Q in the case of Pseudoplastic fluid flow. Figure 7a,b indicates the existence of trappings in the flow. They show that the rise in flow rate causes to increase in the size of vorticed produces during the flow.

Conclusions

In this study, we have considered the flow of heated Rabinowitsch fluid across an elliptical cross section duct. The flow is studied with sinusoidally vibrating walls of the conduit. The impact of physical constraints on Pseudoplastic and Dilatant fluids through elliptic duct is analyzed. A novel mathematical technique is introduced to solve the partial differential equation that includes the heat transfer in present analysis. A polynomial of order six with ten constants is introduced first time in such analysis to solve the temperature equation. The major outcomes of our study are following:

The velocity of flow has same magnitude on the axis of conduit.
The flow velocity decreases rapidly in neighboring of walls for Dilatant fluid than Pseudoplastic fluid.
The temperature has opposite behavior for Pseudoplastic and Dilatant fluids.
Our major task was to solve the complex partial differential equation involved in convection heat transfer and we have provided an exact solution for temperature equation by considering a polynomial of order six with ten constants. Such a polynomial is considered first time in this work to solve the energy equation exactly.
The pressure gradient shows the periodic behavior.
The pressure rise nature of Dilatant fluid opposes the behavior of pressure rise of Pseudoplastic fluid.
The velocity and temperature profiles are parabolic in nature for Pseudoplastic fluid.
The streamlines analysis unfolds that size of trappings reduces with rise in flow rate for Pseudoplastic fluid but has opposite behavior for Dilatant fluid.

References

1. Böhme, G. & Friedrich, R. Peristaltic flow of viscoelastic liquids. *J. Fluid Mech.* **128**, 109–122 (1983).
2. Siddiqui, A. M. & Schwarz, W. H. Peristaltic flow of a second-order fluid in tubes. *J. Nonnewton. Fluid Mech.* **53**, 257–284 (1994).
3. Eytan, O., Jaffa, A. J. & Elad, D. Peristaltic flow in a tapered channel: application to embryo transport within the uterine cavity. *Med. Eng. Phys.* **23**(7), 475–484 (2001).
4. Tsiklauri, D. & Beresnev, I. Non-Newtonian effects in the peristaltic flow of a Maxwell fluid. *Phys. Rev. E* **64**(3), 036303 (2001).
5. Ramachandra Rao, A. & Mishra, M. Nonlinear and curvature effects on peristaltic flow of a viscous fluid in an asymmetric channel. *Acta Mech.* **168**(1), 35–59 (2004).
6. Reddy, M. S., Mishra, M., Sreenadh, S. & Rao, A. R. Influence of lateral walls on peristaltic flow in a rectangular duct. *J. Fluids Eng.* **127**, 824–827 (2005).
7. Tripathi, D., Pandey, S. K. & Das, S. Peristaltic flow of viscoelastic fluid with fractional Maxwell model through a channel. *Appl. Math. Comput.* **215**(10), 3645–3654 (2010).
8. Ali, N., Sajid, M., Javed, T. & Abbas, Z. Heat transfer analysis of peristaltic flow in a curved channel. *Int. J. Heat Mass Transf.* **53**(15–16), 3319–3325 (2010).
9. Akbar, N. S. Entropy generation and energy conversion rate for the peristaltic flow in a tube with magnetic field. *Energy* **82**, 23–30 (2015).
10. Maraj, E. N. & Nadeem, S. Application of Rabinowitsch fluid model for the mathematical analysis of peristaltic flow in a curved channel. *Zeitschrift für Naturforschung A* **70**(7), 513–520 (2015).
11. Hayat, T., Rafiq, M., Ahmad, B. & Asghar, S. Entropy generation analysis for peristaltic flow of nanoparticles in a rotating frame. *Int. J. Heat Mass Transf.* **108**, 1775–1786 (2017).
12. Rashid, M., Ansar, K. & Nadeem, S. Effects of induced magnetic field for peristaltic flow of Williamson fluid in a curved channel. *Physica A* **553**, 123979 (2020).
13. Saleem, A. *et al.* Mathematical computations for peristaltic flow of heated non-Newtonian fluid inside a sinusoidal elliptic duct. *Phys. Scr.* **95**(10), 105009 (2020).
14. McCash, L. B. *et al.* Novel idea about the peristaltic flow of heated Newtonian fluid in elliptic duct having ciliated walls. *Alex. Eng. J.* **61**(4), 2697–2707 (2021).
15. Asha, S. K. & Beleri, J. Peristaltic flow of Carreau nanofluid in presence of Joule heat effect in an inclined asymmetric channel by multi-step differential transformation method. *World Sci. News* **164**, 44–63 (2022).
16. Riaz, A., Awan, A. U., Hussain, S., Khan, S. U. & Abro, K. A. Effects of solid particles on fluid-particulate phase flow of non-Newtonian fluid through eccentric annuli having thin peristaltic walls. *J. Therm. Anal. Calorim.* **147**(2), 1645–1656 (2022).
17. Vaidya, H., Rajashekhar, C., Manjunatha, G. & Prasad, K. V. Peristaltic mechanism of a Rabinowitsch fluid in an inclined channel with complaint wall and variable liquid properties. *J. Braz. Soc. Mech. Sci. Eng.* **41**(1), 1–14 (2019).
18. Gudekote, M. *et al.* Influence of variable viscosity and wall properties on the peristalsis of Jeffrey fluid in a curved channel with radial magnetic field. *Int. J. Thermofluids. Sci. Tech* **7**(2), 1–16 (2020).
19. Vaidya, H., Rajashekhar, C., Manjunatha, G. & Prasad, K. V. Rheological properties and peristalsis of Rabinowitsch fluid through compliant porous walls in an inclined channel. *J. Nanofluids* **8**(5), 970–979 (2019).
20. Manjunatha, G., Basavarajappa, K. S., Thippeswamy, G. & Hanumesh, V. Peristaltic transport of three layered viscous incompressible fluid. *Global J. Pure Appl. Math.* **9**(2), 93–107 (2013).
21. Vaidya, H., Rajashekhar, C., Manjunatha, G. & Prasad, K. V. Effect of variable liquid properties on peristaltic flow of a Rabinowitsch fluid in an inclined convective porous channel. *Eur. Phys. J. Plus* **134**(5), 1–14 (2019).
22. Manjunatha, G., Rajashekhar, C., Vaidya, H., Prasad, K. V. & Makinde, O. D. Effects wall properties on peristaltic transport of Rabinowitsch fluid through an inclined non-uniform slippery tube. *Defect Diffus. Forum* **392**, 138–157 (2019).
23. Nadeem, S. & Akram, S. Heat transfer in a peristaltic flow of MHD fluid with partial slip. *Commun. Nonlinear Sci. Numer. Simul.* **15**(2), 312–321 (2010).
24. Akbar, N. S. & Butt, A. W. Carbon nanotubes analysis for the peristaltic flow in curved channel with heat transfer. *Appl. Math. Comput.* **259**, 231–241 (2015).
25. Bibi, A. & Xu, H. Entropy generation analysis of peristaltic flow and heat transfer of a Jeffery nanofluid in a horizontal channel under magnetic environment. *Math. Probl. Eng.* **2019**, 1–13 (2019).
26. Raza, M. *et al.* Enhancement of heat transfer in peristaltic flow in a permeable channel under induced magnetic field using different CNTs. *J. Therm. Anal. Calorim.* **140**(3), 1277–1291 (2020).
27. Abd-Alla, A. M., Abo-Dahab, S. M., Abdelhafez, M. A. & Thabet, E. N. Effects of heat transfer and the endoscope on Jeffrey fluid peristaltic flow in tubes. *Multidiscip. Model. Mater. Struct.* **17**(5), 895–914 (2021).
28. Abbasi, A., Farooq, W., Khan, S. U., Amer, H. & Khan, M. I. Electroosmosis optimized thermal model for peristaltic flow of with Sutterby nanoparticles in asymmetric trapped channel. *Eur. Phys. J. Plus* **136**(12), 1–18 (2021).
29. Li, P. *et al.* Hall effects and viscous dissipation applications in peristaltic transport of Jeffrey nanofluid due to wave frame. *Colloid Interface Sci. Commun.* **47**, 100593 (2022).
30. Arooj, A., Javed, M., Imran, N., Sohail, M. & Yao, S. W. Pharmacological and engineering biomedical applications of peristaltically induced flow in a curved channel. *Alex. Eng. J.* **60**(6), 4995–5008 (2021).
31. Qayyum, M. *et al.* On behavioral response of 3D squeezing flow of nanofluids in a rotating channel. *Complexity* **2020**, 1–16 (2020).
32. Javed, M., Imran, N., Arooj, A. & Sohail, M. Meta-analysis on homogeneous-heterogeneous reaction effects in a sinusoidal wavy curved channel. *Chem. Phys. Lett.* **763**, 138200 (2021).
33. Qayyum, M. *et al.* Numerical exploration of thin film flow of MHD pseudo-plastic fluid in fractional space: Utilization of fractional calculus approach. *Open Phys.* **19**(1), 710–721 (2021).
34. Zeeshan, A., Ijaz, N., Bhatti, M. M. & Mann, A. B. Mathematical study of peristaltic propulsion of solid–liquid multiphase flow with a biorheological fluid as the base fluid in a duct. *Chin. J. Phys.* **55**(4), 1596–1604 (2017).
35. Hayman, W. K. & Shanidze, Z. G. Polynomial solution of partial differential equations. *Method. Appl. Anal.* **6**, 97–108 (1999).

Author contributions

SA has part in writing original draft and calculations, graphs, results, solutions.MHS has part in writing original draft, calculations, results, solutions.SN has part in conceptualization, supervision.AUW has part in writing, validation of results, software part.S Almutairi has his role in revision of manuscript and writing draft.HA Ghazwani has his role in visualization and formal review of manuscript.MM Sayed has his part in the revision of manuscript and writing original draft.

Competing interests

The authors declare no competing interests.

Additional information

Correspondence and requests for materials should be addressed to S.A.

Reprints and permissions information is available at www.nature.com/reprints.

Publisher's note Springer Nature remains neutral with regard to jurisdictional claims in published maps and institutional affiliations.